DESIGN OF AN ENTRY SYSTEM FOR CARGO DELIVERY TO MARS

Robert Thompson, Larry Cliatt, Chris Gruber, Bradley Steinfeldt[(1)]
Tommy Sebastian, Jamie Wilson[(2)]

[(1)]*Georgia Institute of Technology, 270 Ferst Drive Atlanta Ga. 30332 USA. Email:r.w.thompson@gmail.com*
[(2)]*National Institute of Aerospace/NCSU, 100 Exploration Way Hampton Va. 23666 USA. Email:tsebast@ncsu.edu*

ABSTRACT

Long-term human missions to Mars will require the supply of consumables such as food, water, and oxygen. A sustained campaign of Mars exploration, in which astronauts are on the surface for months to years at a time, may require regular supply missions.

In this paper, a systems study for an entry vehicle for human resupply cargo delivery to Mars is outlined. The design objectives for such a mission might be to deliver 20 metric tons (MT) of human resupply cargo to the surface of Mars at 0 km altitude (MOLA reference) with a landed accuracy of less than 1 km. The system-level trade studies and configurations considered are discussed and a baseline configuration that satisfies the design objectives is presented. Vehicle analysis includes subsystem mass estimation, propulsion sizing, trajectory simulation, aerothermal analysis, thermal protection system sizing, and cost estimation. Uncertainty analysis is performed through Monte Carlo simulation, and the vehicle is sized to achieve the mission requirements to at least a 99% confidence. Uncertainty in entry parameters is modeled. Additionally, technological development required to enable such a mission is discussed.

1. BACKGROUND AND INTRODUCTION

The goals of performing human missions to Mars and sending increasingly large robotic payloads has been existed since human exploration of space began. As such, studies of the design of an entry, descent, and landing (EDL) system for large Mars payloads go back to the 1960s. Under a contract from NASA, the Philco Corporation performed a study on the requirements for a manned Mars Excursion Module (MEM) to deliver two crewmembers and a one ton scientific payload to the Mars surface for a period of 40 days during the 1970-75 timeframe [1].

A more recent example is the NASA Design Reference Mission 3.0 (DRM 3.0) [2]. The DRM 3.0 has been through several iterations as a baseline concept for a possible future human mission to Mars. The DRM 3.0 includes the design of a 10 m diameter, biconic entry vehicle for the delivery of habitats to the surface of Mars. The biconic shape was chosen because of the dimensions and volume restrictions of the habitats, as well as diameter constraints dictated by the launch vehicle used. The architecture outlined by the DRM 3.0 utilizes aerocapture as opposed to direct entry to reduce mass relative to propulsive orbit insertion. The DRM 3.0 uses four supersonic parachutes deployed at Mach 3 and 632 m/s of terminal landing propulsion provided by four RL-10 class LOX/Methane engines [2].

A similar study by Christian, et al. in 2006 discussed landing approximately 25 MT of payload to the Mars surface with initial masses on the order of 100 MT. Again, the mission design utilized an aerocapture into orbit, this time with a 15 m Apollo-like aeroshell capable of a lift-to-drag ratio of 0.3. The aeroshell will be used both for aerocapture and descent; however, it was discussed that two separate heatshields be used in order to avoid the thermal protection system (TPS) material paneling required in order to construct a shield large enough to withstand the heating for both stages of the mission[3]. It was also suggested that no parachute be used. This was based on the conclusion that for masses of this magnitude the mass savings for using a parachute compared to using additional propellant during the final propulsive maneuver (a LOX/Methane rocket system) were insignificant [3].

Based on the information gained from previous design studies, a design methodology was established that would consider the relevant trades to be performed. The baseline architecture was determined and analyzed, based on tools for subsystem mass estimation, propulsion sizing, trajectory simulation, aerothermal analysis, and TPS sizing. Uncertainty in atmospheric density, vehicle mass, aerodynamics, and entry state were analyzed using Monte Carlo analysis to quantify the confidence level of meeting the objectives.The technologies necessary to meet the mission objectives were outlined and their current state of development was discussed. Systems that require technical development in order to accomplish the mission objectives include IAD, supersonic propulsion, in-space assembly of a thermal protection system, or large diameter launch vehicle fairings. Furthermore, facilities and procedures to test and qualify these systems will need to be developed to enable such a mission.

2. APPROACH

2.1 Design Methodology

Three principle trade studies were performed: aeroshell configuration, aerocapture versus direct entry, and mode of deceleration. These trade studies were compared qualitatively through their respective advantages and disadvantages, and quantitatively through their performance in simulation.

For each configuration, aerodynamic analysis and trajectory simulation was performed. The trajectory simulation calculated the amount of propellant required to hit the guidance target on the surface with a 99% confidence. This propellant mass was used to estimate the vehicle dry mass and entry mass through parametric sizing relationships, as well as propulsion system performance to maintain a sufficient thrust-to-weight. Iteration between the weights and sizing analysis and trajectory simulation was repeated until convergence was achieved. Thermal protection system sizing was performed based upon the simulated trajectory, as well as the selection of TPS material that meets the requirements. This process is shown graphically in Figure 1. The converged vehicle was then checked against the original design objectives to ensure that they were met. Several vehicles were converged at different diameter choices, and the vehicle with the smallest gross mass was selected. Because of the computational time involved in evaluating each design point (due to convergence and analyzing uncertainty), optimization of design variables was not performed.
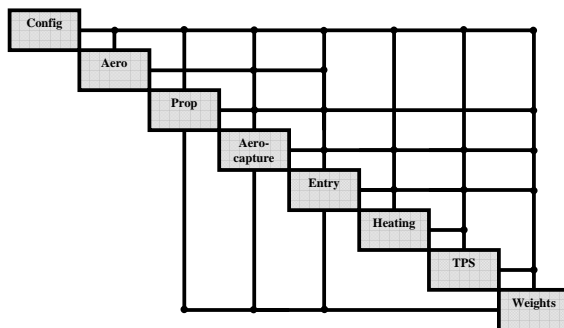

Figure 1 - Design Structure Matrix.

2.2 Tools Used

Trajectory Simulation

A simulator which numerically integrated the set of three degree-of-freedom equations of motion was created to analyze the aerocapture and entry system trajectory. The equations of motion implement modified Newtonian aerodynamics for the hypersonic phases of flight and linearized compressible flow theory for other regimes. Equations of motion describing the trajectory of the vehicle were modified based on the fundamental set derived by Buseman, Vinh, and Culp [4] to include other accelerations along each of the body axes along with variable mass.

A nominal atmosphere based on the northern, mid-latitude, summer atmosphere described in Seiff [5] was modeled and used in the simulation. Winds were defined by Kaplan [6] with constant magnitude equal to the value at 40 km assumed above 40 km. The wind direction was assumed to be westerly throughout the aerocapture and entry. Throughout the entry trajectory, events such as IAD inflation, heatshield jettison, IAD jettison, and backshell jettison were accounted for by changing both the mass and aerodynamics of the vehicle appropriately. Additionally, a mach-number-trigger for propulsive descent was included.

The terminal descent phase of flight implements closed-loop guidance based on work performed by D'Souza [7]. In his work, D'Souza derived an optimal two-point boundary problem guidance law which minimizes the fuel expenditure based on linear variations in the states and a free time-to-go before touchdown. Dispersed values of the initial state, vehicle properties, and atmospheric properties were included for Monte Carlo analysis to ensure the designed system is capable of landing within a 1 km radius for 99% of the analyzed cases.

Weights and Sizing

The vehicle sizing tool used a Weight Breakdown Structure (WBS) to build up the dry mass, margin, entry mass, and aerocapture entry mass. The dry mass elements were calculated with mass estimating relationships from a variety of sources, including historical analogy to vehicles such as Mars Science Laboratory (MSL). The tank mass was based on a volumetric sizing relationship. Because of the uncertainty associated with preliminary mass estimation, a dry mass margin of 40% was used. The sizing accounted for engine scaling based on an engine thrust-to-weight ratio calculated using REDTOP-2 [8]. As an output of the trajectory simulation, the sizer calculated the required thrust to meet a vehicle thrust-to-weight ratio (100% throttle at propulsion start). The payload of the vehicle was assumed to be a human resupply cargo with a density equal to that of the cargo carried by a Progress Module for ISS resupply missions. The progress module carries 1,340 kg in a volume of 4 m^3, resulting in a payload density of 335 kg/m^3 [9].

Propulsion

The propulsion system was analyzed with the REDTOP-2 [8] code developed by SpaceWorks

Engineering Inc. REDTOP-2 is a conceptual rocket engine sizing tool. The user may specify a cycle (such as pressure fed, staged combustion, expander), chamber pressure, oxidizer-fuel ratio, thrust level, and expansion ratio. The software then outputted an engine length, specific impulse, thrust-to-weight ratio, and exit area. This information was then used in the sizing and trajectory analyses. The nature of REDTOP-2 lends itself to effectively analyzing trade studies in propulsion system selection.

The proposed propulsion system was chosen based on its performance and reliability compared to other concepts. While pressure fed cycles provide a high degree of reliability, their performance is significantly lower than pump fed cycles. In addition, the expander cycle, which provides good performance while being relatively simple, can be restarted multiple times with the addition of solid propellant starter motors. NTO/MMH propellants are chosen based on high performance, proven reliability in planetary applications, as well as their storability (they are not susceptible to boil-off).

Aerothermal Analysis and TPS Sizing

By making some key assumptions the TPS mass required could be approximated. The TPS thickness along the body was sized in proportion to the heat rates experienced at each point, compared to the stagnation point heat rate using a cosine variation. However, on large vehicles such as those studied, the maximum heat rate may be experienced elsewhere on the heatshield due to transition to turbulence. To account for this, margin was included in the TPS mass estimation.

The stagnation-point, laminar convective and radiative heating rates were calculated for the Martian atmosphere using the engineering correlations developed by Sutton, Graves, and Tauber [10]. The heating rates were then integrated over the trajectory profile with respect to time, yielding the stagnation-point convective and radiative heat loads.

The selected TPS material was SLA-561, which is an ablative material. It has a relatively low density, yet can withstand fairly significant heating loads compared to other TPS materials that that have been studied [11]. It is also the only TPS material that has been demonstrated on a Mars entry. Surface recession rates were estimated from the heating conditions and integrated with respect to time to yield a total ablation thickness. The thickness of TPS material ablated was then added to the insulation thickness to result in the total TPS thickness. Since the material density and the surface area of the vehicle were known, the required mass of the TPS was determined. The TPS substructure mass was determined using analogy to previous studies [9].

Aerodynamic Analysis

For the scope of this study the analysis of aerodynamics was primarily examined for three different regimes of the EDL: aerocapture, hypersonic, and supersonic flight. Due to the relatively basic shapes of the body at each of these flight regimes, analytically derived aerodynamic analysis were used, including modified Netwonian theory for the hypersonic regimes and linearized compressible theory for the supersonic regime.

3. TRADE STUDIES PERFORMED

Four combinations of aeroshell configuration and mission mode were considered:
- direct entry with blunt body,
- direct entry with lifting body,
- aerocapture and subsequent entry with blunt body, and
- aerocapture and subsequent entry with lifting body.

These options were analyzed starting at the Martian sphere of influence with the same mass and velocity. The mission mode that yielded the most altitude at Mach 5 (the beginning of the supersonic phase of flight, in which parachutes, IADs, or supersonic propulsion may be considered) provides the most timeline margin for the trajectory. The advantages and disadvantages of each vehicle configuration (lifting body versus blunt body) and mission mode (aerocapture versus direct entry) were considered.

3.1 Blunt Body versus Lifting Body

A blunt body such as a 70° sphere-cone has been used on every US mission to Mars that had an EDL component, from Viking to MSL. The advantage to this shape is that it has a comparatively high hypersonic drag coefficient. This results in a smaller ballistic coefficient compared to other shapes with equal mass and reference area. The resulting trajectories experience more deceleration at higher altitudes than higher ballistic coefficient trajectories. For a 70 MT entry vehicle with a 14 m diameter flying at an angle of attack of 15 degrees (yielding an L/D of 0.23), the ballistic coefficient is 288 kg/m^2. This is several times higher than any Mars entry vehicle flown to date.

There are several difficulties with the large diameter sphere-cone concept. Perhaps the most significant challenge is launch of the aeroshell. The largest launch vehicle payload fairing in existence for the foreseeable future is the Ares V, with payload diameter of 8.5 m [13]. In all previous Mars missions, the entry vehicle has been contained within the launch vehicle fairing. This would be limiting for the launch of a blunt body

aeroshell because the ballistic coefficient increases significantly with decreased diameter, as shown in Figure 2. The entry mass of the vehicle was allowed to scale, keeping payload mass and propellant mass fraction constant.
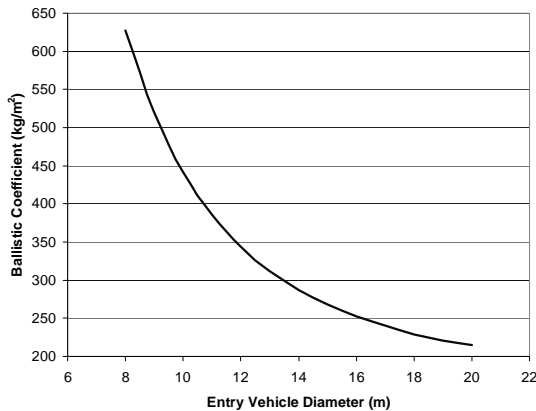

Figure 2 - Blunt Body Ballistic Coefficient versus Diameter (Fixed Drag Coefficient).

Ballistic coefficients in the 500-600 kg/m^2 range result in trajectories that decelerate deep in the atmosphere, leaving the entry vehicle little timeline margin. Therefore, entry vehicles with diameters larger than 10 m must be considered (unless a hypersonic IAD is used to increase the drag area on entry, which may inhibit the ability to use hypersonic guidance). There are two options for launching such a vehicle: launch it in pieces and assemble it on-orbit or develop a hammer-head style payload adapter in order to launch the larger diameter vehicle on an existing rocket. On-orbit options will require either the presence of astronauts or the development of advanced robotic systems. In the near-term, human assembly is the most likely option to be considered. Involving astronauts adds significantly to the expense and risk of the mission by adding additional launch and rendezvous operations to the mission profile. Therefore the lower risk and potentially lower cost option would be the design of a special hammer-head style payload adapter for an existing launch vehicle. The disadvantages of such a design would be in aerodynamic performance. The extent of this reduced performance has not been studied in detail for the Ares V, but it is likely that the remaining performance would be sufficient to launch the entirety of the entry vehicle in a single launch. The excellent drag performance of blunt bodies make them a good option for the growth of entry vehicles at Mars to accommodate very large payloads in the 20 MT range, in the event that the challenges identified can be resolved.

A bi-elliptic vehicle, also known as an ellipse-sled has been proposed as a concept for Earth and Mars entry vehicles. An example is shown in Figure 3. The advantage of the shape is that when flown at angle of attack, it generates a significant lift compared to drag that can be used to achieve greater cross range and targeted hypersonic guidance through bank angle modulation than is possible with a blunt body at angle of attack. The disadvantage of this class of slender lifting bodies is that there is a reduction in hypersonic drag coefficient by about a third when compared to the blunt body and convective heating is increased due to a reduced effective nose radius. Because the hypersonic drag coefficient is crucial in determining the ballistic coefficient and the trajectory the vehicle will fly, this is an important effect.

Figure 3 – Ellipsled Configuration [14].

The advantage of the lifting body is that it may more easily fit onto a launch vehicle. Previous studies have considered lifting bodies with diameters around 10-12 m. Trajectory simulations were performed flying the ellipsled at an angle of attack of 29 deg, resulting in a total L/D = 1 and C_D = 0.867. Direct entry and entry from Mars orbit is complicated by this configuration, due to its low drag area. Because of its high L/D, the vehicle tends to skip out of the atmosphere over a wide range of flight path angles when flown lift-up without hypersonic guidance. A hypersonic guidance algorithm utilizing bank angle modulation can be used to prevent this.

The reduced drag area (and corresponding increase in ballistic coefficient) means that the vehicle will decelerate lower in the atmosphere than a blunt body (with lower ballistic coefficient) would. There are several ways to compensate. First, a larger supersonic decelerator can be used. This can include an IAD deployed below Mach 5 or a supersonic parachute deployed below Mach 3. Another option is providing additional propulsive capability, through the use of a higher thrust-to-weight engine and a higher propellant mass fraction. Each of these options uses additional mass that otherwise could have been allocated to payload.

3.2 Direct Entry versus Aerocapture

Every Mars entry since Pathfinder has utilized a direct entry, in which the entry vehicle performs EDL without first going into orbit around the planet. This results in entry velocities around 6 km/s, depending on the Earth-Mars trajectory. This large entry velocity results in significantly higher heat rates and heat loads than entry from low Mars orbit; however, direct entry has the benefit of not requiring extra heat shields,

deployable decelerators, or propulsion for an insertion maneuver, possibly resulting in lower mass and complexity.

Direct entry with both a blunt body (L/D = 0.23) and a slender lifting body (L/D = 1) were considered. Entry mass was assumed to be 70 MT for both vehicles, which is based on initial weights and sizing estimates. The blunt body flew a trajectory that took it to Mach 5 at 10 km altitude. This altitude helps determine how much time will be left for performing supersonic deceleration. This can be thought of as a surrogate for landed accuracy as with increased timeline more maneuvers are possible to target the landing site.

On the other hand, the slender body has a tendency to exit the atmosphere when the trajectory was flown lift-up. When flown at a constant bank angle of 85°, the slender body was able to stay in the atmosphere, but due to its low hypersonic drag coefficient, the Mach 5 transition altitude is at 6 km, leaving little timeline margin for the rest of deceleration. When bank angle is set back to 0° once entry is assured, this transition altitude can be increased; the downside to this class of trajectory is that heat rates and heat loads are high compared to other trajectories and vehicle configurations.

Aerocapture involves entering the atmosphere from a hyperbolic trajectory and using drag to slow the vehicle down enough to exit the atmosphere in a closed orbit around Mars. Previous studies have shown that aerocapture can lead to a mass and cost savings over other options including direct entry, aerobraking, and propulsive insertion. Aerocapture reduces the kinetic energy of the entry vehicle by 20-40% at entry atmospheric interface. Entry from this slower velocity reduces the severity of the heating environment experienced by the vehicle, allowing for a thermal protection system mass savings. This strategy also allows the entry vehicle to reach Mach 5 at a higher altitude compared to direct entry.

The performance advantages that aerocapture provides must be weighed against the operational disadvantages. With two entry sequences, any errors in orbit after the aerocapture trajectory must be detected and corrected to ensure that the entry sequence begins as planned. The heat imparted to the heatshield on the aerocapture pass also must be dealt with. Nested dual heatshields have been proposed, in which the aerocapture heatshield is jettisoned after the first pass through the atmosphere with a second heatshield is used on entry [15]. An alternative is the use of a hypersonic IAD during aerocapture. The larger drag area decreases the ballistic coefficient sufficiently that the vehicle decelerates higher in the atmosphere, and sufficiently reduces the heat rates seen on the vehicle. Overall, aerocapture is a more complex mission mode than

direct entry. While these trade studies can be analyzed for their performance at a conceptual level, more detailed studies should be performed to identify the most cost and mass efficient option.

3.3 Supersonic Deceleration

An inflatable aerodynamic decelerator is a deployable structure that increases the drag area of the entry vehicle. IAD inflation up to Mach 5 has been proposed for use at Mars for supersonic deceleration [16]. The advantage of such a device is that it has a relatively high drag coefficient compared with other supersonic decelerators, such as a supersonic parachute. There are two classes of IAD: trailing and attached. The attached IAD has a higher drag area per unit mass than the trailing IAD. The disadvantage is that it can be difficult to integrate with the entry vehicle. Because it provides more drag, the attached IAD will be considered for this application.

Parachutes have been used on all Mars lander missions to date. The technology for Mars supersonic parachutes is qualified up to a Mach 2.2 deployment. Further technology development could push this to Mach 3. Supersonic parachutes, however, have lower drag coefficients than attached inflatable decelerators. This is evident in Figure 4 which shows the drag coefficients for a variety of decelerators over a range of Mach numbers. The comparatively low C_D can be mitigated to some extent by increasing the diameter of the parachute or by clustering parachutes, but both options introduce complexity for development, qualification, and manufacturing. For example, to provide the same drag force as an attached IAD at Mach 3 with a diameter of 25 m, a supersonic parachute would need to have a diameter of 38 m, or be replaced by a cluster of three parachutes with diameters of 23 m each.
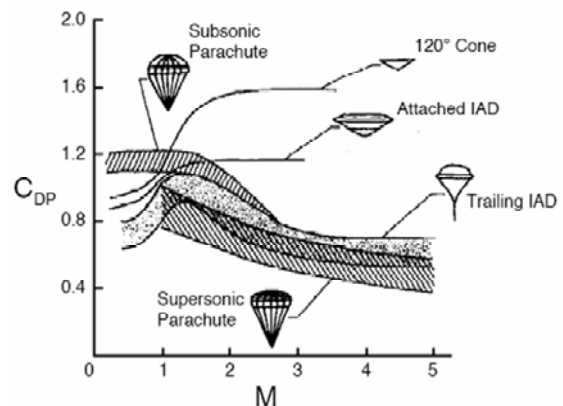

Figure 4 - Decelerator Drag Coefficient versus Mach Number [16].

Propulsion is another option for supersonic deceleration. Studies of all-propulsive landing have

shown that a high propellant mass fraction results when propulsion is the sole supersonic decelerator [15]. In combination with other decelerators, such as an IAD or parachute, propulsion allows an opportunity to eliminate any final guidance errors and approach the target with precision.

3.4 Summary of Trades Studied

Direct entry at 6 km/s.
- Blunt body: With an entry mass of 70 MT and a diameter of 14 m, Mach 5 achieved at 10 km altitude.
- Lifting body: Bank angle modulation required to prevent vehicle from skipping out of the atmosphere. Mach 5 transition altitude of 17 km can be achieved, but heating environment for this trajectory is very severe.

Aerocapture, circularization, entry
- Blunt body: Over a wide range of entry masses, flight path angle, and vehicle diameter, aerocapture into a closed orbit is successful. Mach 5 altitude varies based on entry flight path angle, but a typical result is 15 km. This option provides the highest Mach 5 transition altitude of the trades considered.
- Lifting body: Aerocapture is successful over a range of entry flight path angles, although the vehicle tends to drop very deep into the atmosphere. On entry, the Mach 5 altitude is somewhat lower than the blunt body, at 8 km.

Supersonic Deceleration
- IAD versus Parachute: The IAD concept is the most favorable because it can be deployed at Mach 5. Such early deployment, along with its high drag area, means that it can provide the greater drag impulse than a supersonic parachute.
- Supersonic Propulsion: Because of the high mass ratios, supersonic propulsion was not considered by itself. Propulsion, however, is required for terminal deceleration and targeted landing. The Mach number for propulsion start is a parameter for optimization that was not explored; for the purposes of this study, it has been assumed to be Mach 2.

4. PROPOSED DESIGN

A blunt body was chosen due to its high hypersonic drag coefficient (resulting in a lower ballistic coefficient), and its ability to achieve moderate amounts of lift by trimming at angle of attack. Because hypersonic guidance was not simulated in this study, the full range of possibilities of a slender body were not determined; however, the trajectories they fly will tend to have more severe heating environments as they decelerate lower in the atmosphere due to a lower

ballistic coefficient. This results in a higher TPS mass fraction than other concepts. The diameter of 14 m was chosen by trading vehicle mass with deceleration performance.

Aerocapture with a nested heatshield was selected over direct entry, due to the reduction in heat rates experienced. The ability to utilize a check-out period in orbit also mitigates some risk of entering during periods of inclement weather, such as dust storms. However, this comes at the expense of increased development and operational cost, as well as increased complexity in the nested heat shield.

In the interest of beginning supersonic deceleration as early as possible, an attached IAD was selected rather than a supersonic parachute, due to the potential to deploy an IAD as high as Mach 5. Guided propulsion is initiated at Mach 2 in order to provide terminal descent and guide the vehicle to its final landing site. The selected architecture is shown in Figure 5 and Figure 6.
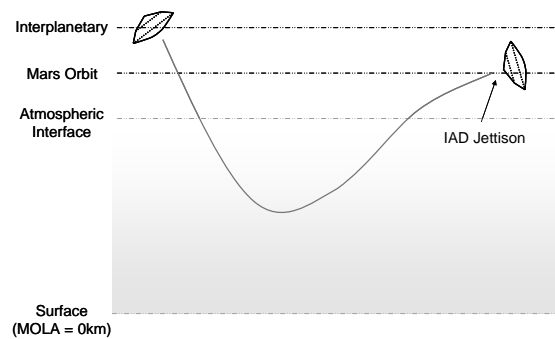

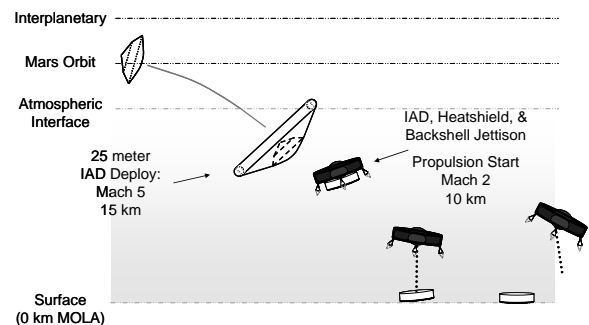Figure 5 - Aerocapture Sequence.

Figure 6 - Entry, Descent, and Landing Sequence.

4.1 Aerocapture

The mission begins at Mars with an approach from a hyperbolic orbit. The incoming hyperbolic excess velocity is assumed to be 3.317 km/s. An entry flight path angle of 8.5° was chosen based on trajectory trade studies, and the resulting entry velocity is 5.96 km/s. The aerocapture system is designed to handle uncertainty in entry velocity and flight path angle.

After aerocapture, the vehicle leaves the atmosphere and using reaction control system (RCS) propellant executes a periapsis raising maneuver. When the vehicle is in position for deorbit, another propulsive burn puts the spacecraft on the appropriate trajectory to enter the atmosphere at the desired altitude, flight path angle, and velocity.
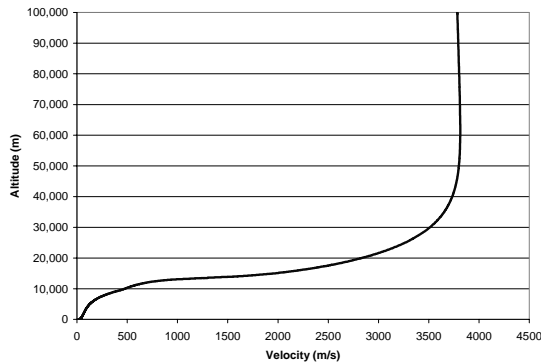

Figure 7 - Entry Trajectory.

4.2 Entry

The nominal entry trajectory is shown in Figure 7. The vehicle initiates its entry sequence upon contact with the Martian atmosphere, which marks the beginning of its hypersonic entry phase. As the literature review suggested, it was assumed that a guidance algorithm utilizing lift modulation during the hypersonic phase was necessary to achieve precision landing accuracy. The entry vehicle is flown with an L/D = 0.23 until IAD deployment.

Table 1 - Heating and TPS.

Entry Heating at Stagnation Point	
Peak Convective Heat Rate	19.67 W/cm^2
Altitude at Peak Convective Heat Rate	26.3 km
Peak Radiative Heat Rate	3.13 W/cm^2
Altitude at Peak Radiative Heat Rate	16.0 km
Integrated Heat Load	1,752.4 J/cm^2
Entry TPS Mass + 40% Margin	468.72kg
Aerocapture Heating at Stagnation Point	
Peak Convective Heat Rate	18.03 W/cm^2
Altitude at Peak Convective Heat Rate	53.8 km
Peak Radiative Heat Rate	0.08 W/cm^2
Altitude at Peak Radiative Heat Rate	51.8 km
Integrated Heat Load	1,723.3 J/cm^2
Entry TPS Mass + 40% Margin	473.20 kg

4.4 IAD Deceleration

At Mach 5, the supersonic IAD is deployed. It is inflated with a combination of ram-air and helium inflation gas. A 25 meter attached IAD was used in this study; this diameter can be traded against propellant for propulsive terminal descent. A larger IAD imparts more drag force on the vehicle, subsequently requiring less propellant. However, a larger IAD is heavier and will be more difficult to qualify. Following IAD deployment, ballistic flight was assumed.

4.3 Terminal Landing

After decelerating through the high supersonic regime ($2 \leq M \leq 5$), the vehicle enters the terminal descent regime of flight. The initiation of the terminal descent is marked by the heatshield being ejected from the rest of the system, allowing the propulsion system located on the descent stage to initiate. The ballistic coefficient of the heatshield, as compared to the entry vehicle with the supersonic IAD still attached, is sufficiently high that recontact is not a concern. After heatshield separation, the backshell and supersonic IAD are shed, and guided propulsive descent begins. A thrust-to-weight ratio of 2.2 at beginning of propulsive descent was used. The guidance law for the propulsive descent ensures that the desired end state is achieved and implements a modified version of a closed-loop guidance algorithm developed by D'Souza. Throughout the propulsive descent, the vehicle throttles its engines so that the net direction and magnitude of the thrust vector is identical to that commanded by the guidance algorithm. The final stage of the terminal descent employs the Skycrane Landing System (SLS) as developed for MSL.

Table 2 – Entry Vehicle Mass Breakdown.

#	Element	Mass
1.0	Body	15,790 kg
2.0	Entry Heat Shield	2,028 kg
3.0	Terminal Descent & Landing	1,918 kg
4.0	Avionics	165 kg
5.0	Power Supply and Distribution	764 kg
6.0	Propulsion	892 kg
7.0	Dry Mass Margin (40%)	8,623 kg
8.0	**Dry Mass**	**30,181 kg**
9.0	Payload	20,000 kg
10.0	**Landed Mass**	**50,181 kg**
11.0	Landing Propellant	17,712 kg
12.0	Inflatable Aerodynamic Decelerator	3,000 kg
13.0	**Entry Mass**	**70,893 kg**
14.0	Deorbit & Circ Propellant	5,085 kg
15.0	Aerocapture Heat Shield	2,704 kg
16.0	**Aerocapture Mass**	**78,683 kg**

5. FEASIBILITY ANALYSIS

Monte Carlo simulations are performed to assess the ability of the vehicle to meet the requirement of landing within a 1 km radius of the landing site 99% of

the time. Dispersions due to vehicle state and aerodynamics are assumed to be similar to MSL. The dispersions on state and vehicle parameters can be seen in

Table 3 for the aerocapture and entry trajectory, respectively. The dispersed entry state values are conservative estimates and meet or exceed the errors expected for MSL's direct entry.

Table 3 - Monte Carlo Variations for Aerocapture and Entry [18].

	Parameter	Nominal	Distribution	3σ or min/max
A/C State	Aerocapture Velocity	5985 m/s	Gaussian	6 m/s
A/C State	Aerocapture Flight Path Angle	-8.5°	Gaussian	0.11°
Entry State	Entry Velocity	3789 m/s	Gaussian	6 m/s
Entry State	Entry Flight Path Angle	-11°	Gaussian	0.11°
Vehicle	Aerocapture Mass	78,683 kg	Gaussian	72.0 kg
Vehicle	Entry Mass	70,890 kg	Gaussian	64.5 kg
Vehicle	Engine Thrust	515kN	Uniform	+/- 5%
Vehicle	Engine Specific Impulse	387 s	Uniform	+/- 0.67%
Vehicle	CA Multiplier (M>10)	1	Gaussian	3%
Vehicle	CN Multiplier (M>10)	1	Gaussian	5%
Vehicle	CA Multiplier (0.8<M<5)	1	Gaussian	10%
Vehicle	CN Multiplier (0.8<M<5)	1	Gaussian	8%
Vehicle	CA Multiplier (M<0.8)	1	Gaussian	5%

Atmospheric dispersions were obtained by assuming a uniform variation between the cool, low-pressure and the warm, high-pressure atmospheres cited in Seiff [5]. The atmosphere was assumed to have a uniform distribution between the maximum and minimum values with properties being calculated at every time step. This represents increased *a priori* climate knowledge prior to the aerocapture phase of flight, which requires an orbiter with instrumentation such as the Mars Climate Sounder (providing atmospheric density profiles) to exist at the time of the mission [19]. Alternatively, active guidance could be incorporated that can assess the trajectory and target specific atmospheric exit conditions.

Using the dispersions described previously, 500 case Monte Carlo simulations are performed for both the aerocapture and entry portions of flight. For aerocapture, the system was sized to handle the worst case in-space propulsive requirement to set up the appropriate entry conditions. This includes a periapsis raise burn, an apoapsis raise burn, and a deorbit burn. The nominal, best case and worst case propulsive requirements are shown in Table 4.

Table 4 - Best, Nominal, and Worst Case In-Space ΔV.

Best Case	145.40 m/s
Nominal Case	156.66 m/s
Worst Case	263.89 m/s

For the entry phase of flight, two metrics are important: the fuel mass required to achieve the required landing accuracy and the distance from the target landing site. The target for the analysis is assumed to be 40º N, 96º W, a 0 km MOLA site located in the Alba Patera region of Mars. At the Mach 5 IAD deployment, the dispersions modeled resulted in a scatter of 23 km in semi-major axis, and an altitude distribution between 13 and 16 km. The use of a guidance algorithm in the hypersonic regime can reduce this error.

In the simulation used in this study, however, terminal descent guidance was able to meet the 1 km requirement with 99% confidence from the dispersed Mach 5 IAD deployment point. This propulsive maneuver requires a maximum of 15011 kg propellant, and maximum a miss distance of 437 m. The amount of propellant is covered adequately by the baseline, which provides 18% margin on descent propellant. However, no navigational errors are modeled; therefore the true target miss distance will be larger. Studies have shown, however, that the accumulated navigational error should not exceed 450 m [20]. The simulation also did not account for the SLS landing; it assumed that a vertical descent phase negates the residual velocity after arriving at the target. With respect to the errors modeled, the simulation achieves its target greater than 99% of the time.

6. TESTING AND QUALIFICATION

Many of the technologies proposed in this study involve significant departures from heritage systems. MSL represents the limit to which Viking heritage can reach [21]. New technologies must be tested and validated if future missions that seek improvement over previous endeavors are to succeed. In that respect, the system qualification costs proposed by this study should be viewed as costs toward the development of a new Mars EDL heritage, and is therefore an investment in the success of future missions. As with all technologies, testing costs increase substantially when the payload is human rather than robotic [21]. Of the proposed technologies, the two most underdeveloped are the large-diameter IADs used for aerocapture and supersonic deceleration and the on-orbit assembly of the TPS.

Current inflatable decelerator analysis methods are similar to the methods used with parachutes. Both rely on empirical data and both allow for scaling of results; however, the methods are poorly understood and have not been validated. A series of tests must be carried out to understand the decelerator behavior and characteristics. Qualification must establish that the IAD will deploy correctly, that it will inflate successfully, and that it will provide the expected drag

and stability once inflated [22]. Testing of inflatable decelerators on the scale proposed by this study has

Test Name	Description	Objectives
Wind Tunnel Test Program	Scale vehicle model in different IAD configurations	1) Develop aerodynamic database 2) Determine aerodynamic coefficients 3) Measure the drag force as a function of M and ρ 4) Demonstrate the viability of supersonic propulsion 5) Determine the effect of propulsive exhaust on flowfield and vehicle heating
Scaled Rocket Testing	Deploy scale model of vehicle from a sounding rocket at high altitude and Mach number to simulate entry conditions	1) Collect data on the dynamic stability of the scaled vehicle 2) Validate the deployment method of the IADs 3) Study the IAD/aeroshell interaction during deployment 4) Compare results to other analysis methods
Balloon Drop Testing	Deploy full-scale model of the vehicle from a sounding rocket, first carried by a balloon, at high altitude and Mach number to simulate entry conditions	1) Collect data on the dynamic stability of the full-scale vehicle 2) Validate the deployment method of the IAD 3) Study the IAD/aeroshell interaction during deployment 4) Compare results to other analysis methods
Radiative Lamp Testing	Supersonic wind tunnel used in combination with radiative lamps to simulate entry conditions experienced by IAD materials	1) Determine the robustness of IAD materials 2) Demonstrate packed IAD can perform acceptably under simulated entry conditions once deployed
Arc-plasma Jet Testing	Test coupons of TPS material at high enthalpy conditions similar to entry	1) Determine the maximum heating limits of the TPS material 2) Determine back-surface temperature gradient over simulated entry 3) Optimize design of "tortuous path" for TPS panel joints
On-Orbit Assembly Demonstration	Assembly and testing of mock heatshield at ISS	1) Demonstrate on-orbit assembly capability through spacewalks 2) Test heatshield validity through Earth entry
Gantry Testing	Skycrane supported by gantry will be tested for stability and controller robustness	1) Demonstrate skycrane and bridle design can support landing loads 2) Validate control algorithm, specifically during touchdown

Table 5 - Testing and Qualification.

never been carried out. There are no existing facilities capable of testing the decelerators at full-scale at the appropriate atmospheric conditions and Mach numbers. Ground based testing may be carried out using subscale models at desired velocity and flow conditions. NASA Langley has a wind tunnel that may carry out such a test, but it has a test model limit of 6 in [21]. The model must also be rigid, making fluid-structure interaction observation impossible [22]. Sounding rocket tests may also be carried out to perform tests on a larger scale system. A one-tenth to one-half scale model of the IAD is lifted to approximately 100 km, where the density approximated Martian conditions. Balloon drop tests, like those used to validate the Viking aerodynamic decelerator systems, work in a similar manner [23]. A balloon carries the system to some altitude at which time it is dropped and a rocket accelerates the system to the desired altitude and Mach number; the IAD is then deployed. Because the IADs are attached to the aeroshell, wake effects are not a great concern, so the system can be tested at full scale, but not necessarily full mass, minimizing the testing costs. It may also be possible to piggyback the test on another mission, using the launch vehicle lower stages to carry the system to some high altitude and desired Mach number. Such a test would, however, introduce complexity to the carrier mission, and further testing would have to be carried out to ensure the safety of the carrier mission. The IAD material also needs to be tested for robustness (ability to successfully inflate after long-term storage) and for its ability to withstand heating loads. The low heating rate experienced by the

material (relative to the stagnation point) allows for more testing options, like using radiative lamps in a supersonic facility to model flight conditions [24].

The selected TPS material, SLA-561, has a significant amount of data describing its behavior in a variety of flight conditions. Its use in paneling together a heatshield, however, has not been intensively studied. There are significant risks associated with assembling a heatshield in this fashion, namely, creating direct pathways of high-temperature gas to the back-surface. TPS panels must be joined in such a way that the panel interfaces form a "tortuous path" for on-coming flow, minimizing the risk to the back-surface [25]. Arc plasma testing of coupons manufactured using such joints can qualify manufacturing and assembly techniques to as close to flight conditions as possible without actually performing a flight test [24]. Flight tests of scale models, employing paneled heatshields, can be executed using sounding rockets, providing insight into how the material will ablate and if the joints behave as weak spots, promoting spalation or flow bypass. PICA, a TPS material that will accommodate paneling, is another option.

There are other technologies that require validation. The skycrane, currently planned for use on MSL, must be tested for a 20 MT landed mass, which is twenty times heavier than MSL. There are a number of ways to validate this system, including gantry and helicopter-suspended tests. Key in the validation of the skycrane will be the demonstrated robustness of the on-board

controller, particularly during the touchdown phase [26]. The successful execution of this system on MSL will also help in decreasing risk associated with new, unproven systems [21]. Supersonic propulsion must also be tested, but first it must be demonstrated. New issues arise with the introduction of supersonic propulsion. Thermal protection must be provided as the vehicle is now enveloped in a high temperature recirculating exhaust. Currently, the most viable form of testing involves subscale tests in supersonic wind tunnels, but flight test experiments at altitude must also be designed to successfully qualify the supersonic propulsion. Aerocapture, another method that has not been demonstrated, has been studied by numerous individuals. Successful execution of aerocapture via drag modulation, for example, must be studied using a six degree-of-freedom analysis tool, like POST [21]. Flight tests can then be carried out, requiring the scale model to start in some high-altitude orbit, and then be accelerated into the atmosphere approaching the orbital escape velocity. Table 5 is a proposed verification and validation program for the key technologies proposed by this study.

8. CONCLUSIONS & FUTURE WORK

This study has demonstrated that cargo delivery to the surface of Mars in support of human exploration can be achieved with an architecture consisting of a blunt body, aerocapture, and inflatable aerodynamic decelerators. Hypersonic guidance and terminal propulsive guidance are identified as important to achieving the landed accuracy requirement. The feasibility of the concept is investigated through the use of Monte Carlo simulation, to demonstrate that conservative estimates in dispersion of vehicle and state parameters result in at least a 99% confidence in achieving the targeted end state. Future studies will include the optimization of the vehicle and trajectory parameters, as well as the consideration of additional inflatable decelerator concepts for aerocapture and entry.

9. ACKNOWLEDGMENTS

9. REFERENCES

1. Dixon, F.P. "An Early Mars Landing Mission Using The Mars Excursion Module." Philco Aeronutronic Division, Newport Beach, CA.
2. "Reference Mission 3.0: Addendum to the Human Exploration of Mars." Johnson Space Center, 1998.
3. Christian, John et al. "Sizing of an Entry, Descent, and Landing System for Human Mars Exploration." AIAA-2006-7427. September 2006.
4. Buseman, A., Vinh, N., and Culp, R., "Solution of the Exact Equations for Three-Dimensional Atmospheric Entry Using Directly Matched Asymptiotic Expansions," NASA CR-2643, 1976.
5. Seiff, A., "Post-Viking Models for the Structure of the Summer Atmosphere of Mars," *Advances in Space Research*, Vol. 2, pp. 3-17, 1982.
6. Kaplan, D. "Environment of Mars, 1988," NASA TM 1000470. 1988.
7. D'Souza, C., "An Optimal Guidance Law for Planetary Landing." Paper No. AIAA 97-3709, 1997.
8. "Rocket Engine Design Tool for Optimal Performance – 2 (REDTOP-2)". Academic Version. SpaceWorks Engineering, Inc. 2005.
9. Wade, Mark. "Encyclopedia Astronautica: Progress M." http://www.astronautix.com/craft/progressm.htm. Accessed March 1, 2007.
10. Sutton, K. and Graves, R. A. "A General Stagnation-Point Convective-Heating Equation for Arbitrary Gas Mixtures". NASA TR R-376. 1971.
11. Williams, S.D. and Curry, Donald M. "Thermal Protection Materials – Thermophysical Property Data". NASA RP-1289. December 1992.
12. Williams, S.D., Pavlosky, J.E., and Curry, D.M. "A Preliminary TPS Design for MRSR – Aerobraking at Mars and at Earth". AIAA-90-0052. January 1990.
13. "Exploration Systems Architecture Study Final Report". NASA-TM-2005-214062. November, 2005.
14. Theisinger, J. Aerodynamics Calculation and Optimization. Pending Georgia Tech Masters Project.
15. Braun, R.D., Manning, R.M., "Mars Exploration Entry, Descent and Landing," *2006 IEEE Aerospace Conference*, IEEEAC #0076, Big Sky, Montana, March 2006.
16. Brown, G., et al. "Hypercone Inflatable Supersonic Decelerator", AIAA-2003-2167, 2003.
17. Gillis, C.L. "Deployable Aerodynamic Decelerators for Space Missions." Journal of Spacecraft. Volume 6 Issue 8. August 1969.
18. Striepe, S.A., Way, D.W., Dwyer, A.M., and Balaram, J., "Mars Science Laboratory Simulations for Entry, Descent, and Landing." Journal of Spacecraft and Rockets. Vol. 43, No. 2, March-April 2006.
19. "Mars Climate Sounder." http://www.planetary.org/programs/projects/mars_climate_sounder/facts.html. Accessed Online April 7 2007.
20. Ely, T.A., Duncan, C., Lightsey, E.G., and Mogensen, A, "Real Time Mars Approach Navigation Aided by the Mars Network." Paper No. AIAA 2006-6565, AIAA GNC Conference, 21-24 August 2006, Keystone, Colorado.
21. Cheatwood, Neil. TPS and Qualification Testing Interview. April 2007.
22. Buck, Gregory M. "Testing of Flexible Ballutes in Hypersonic Wind Tunnels for Planetary Aerocapture". 44th AIAA Aerospace Sciences Meeting and Exhibit Reno, NV. January 2006.

23. Timmons, J. D. "Viking Balloon Launched Decelerator Tests". 27th International Astronautical Congress. Anaheim, CA. October 1976.

24. Laub, B. "Tutorial on Ablative TPS". NASA Ames Research Center. Moffett Field, CA. March 2007.

25. Tompkins, S.S., Pittman, C.M., and Stacey, A.B. "Thermal Performance of a Mechanically Attached Ablator Tile for On-Orbit Repair of Shuttle TPS". NASA TM-81822. May 1980.

26. Mitcheltree, R., Steltzner, A., Chen, A., SanMartin, M., Rivellini, T. "Mars Science Laboratory Entry Descent and Landing System Verification and Validation Program". Pasadena, CA. 2006.